

## Physical, Mechanical, and Tribological Properties of Quasicrystalline Al-Cu-Fe Coatings Prepared by Plasma Spraying

A.A. Lepeshev<sup>1,2</sup>, E.A. Rozhkova<sup>1</sup>, I.V. Karpov<sup>1,2</sup>, A.V. Ushakov<sup>1,2</sup>, L.Yu. Fedorov<sup>1,2</sup>, E.A. Dorozhkina<sup>3</sup>, O.N. Karpova<sup>3</sup>

<sup>1</sup> Siberian Federal University, Krasnoyarsk, 660041 Russia

<sup>2</sup> Krasnoyarsk Scientific Center, Siberian Branch of the Russian Academy of Sciences, Krasnoyarsk, 660036 Russia

<sup>3</sup> Reshetnev Siberian State Aerospace University, Krasnoyarsk, 660014 Russia

E-mail: [sfu-unesco@mail.ru](mailto:sfu-unesco@mail.ru)

**Annotation.** The physical, mechanical, and tribological properties of quasicrystalline coatings based on the Al<sub>65</sub>Cu<sub>23</sub>Fe<sub>12</sub> alloy prepared by plasma spraying have been investigated. The specific features of the phase formation due to the competitive interactions of the icosahedral  $\psi$  and cubic  $\beta$  phases have been elucidated. A correlation between the microhardness and the content of the icosahedral phase in the coating has been determined. The decisive role of the quasicrystalline phase in the formation of high tribological characteristics of the coatings has been revealed and tested.

Quasicrystalline alloys, which are characterized by an unusual quasiperiodic structure and a crystallographically forbidden fivefold symmetry axis, possess a unique set of chemical, physical, and mechanical properties [1-7]. In this respect, noteworthy are quasicrystalline Al-Cu-*Me* alloys (where *Me* is Fe, Cr, Mn, or V) with a relatively small specific weight, which have high values of the chemical durability, elastic modulus, hardness, and wear resistance and a low value of the friction coefficient. The development of compositions and technologies for processing of these alloys has opened up wide possibilities for their use as antifriction materials in friction units. The high efficiency of friction pairs can be achieved both through the use of composites with a quasicrystalline alloy hardener and through the direct deposition of quasicrystalline coatings.

Among the most promising methods for fabricating units from quasicrystalline alloys is powder metallurgy, in particular, plasma spraying [8-21]. The use of technological capabilities of this method makes it possible, during the spraying of quasicrystalline coatings, not only to control their structure and phase composition but also to purposefully form composites with a specified ratio of the base material and quasicrystalline alloy components.

The purpose of this study is to investigate the processes of the structure and phase formation in quasicrystalline coatings under different technological conditions of their deposition and to perform tribological tests of the prepared coatings.

The investigations were performed on samples of coatings deposited on the outer surface of the copper rings using an oscillating plasma torch with coaxial powder injection into the cathode region [9, 10]. The temperature conditions of deposition were controlled by a thermocouple connecting the inner part of the ring and the outer surface. The ligature and initial powders of the Al<sub>65</sub>Cu<sub>23</sub>Fe<sub>12</sub> alloy for plasma spraying were prepared using the gas atomization method. The dispersion of the obtained powders was 25-106  $\mu\text{m}$ .

The main parameters of the plasma spraying of quasicrystalline coatings based on the Al-Cu-Fe alloy are presented in below. Different thermal conditions of plasma spraying of the coatings were provided by varying the temperature of the copper substrate  $T_k$ .

- Arc current 200-250 A
- Power 13-17 kW
- Plasma-forming gas flow rate 0.008-0.0127 kg/s

- Carrier gas flow rate 0.08-0.12 kg/s
- Gas flow rate at the cross section 0.0065 kg/s
- Spraying distance 110-130 mm
- Powder flow rate 0.046-0.056 kg/s

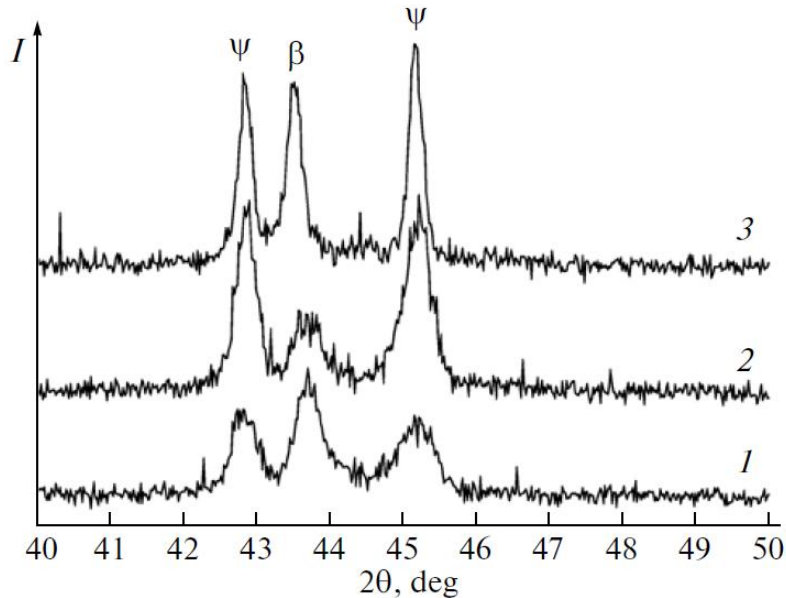


Fig. 1. X-ray diffraction pattern of the  $\text{Al}_{65}\text{Cu}_{23}\text{Fe}_{12}$  quasicrystalline alloy coatings deposited at different temperatures of the substrate  $T_k = (1) 500$ ,  $(2) 650$ , and  $(3) 850^\circ\text{C}$ .

The thickness of the deposited coatings varied in the range from 1.65 to 2.75 mm.

The X-ray structural and powder diffraction analyses of the initial powders and deposited quasicrystalline coatings were performed on a DRON-3 automated diffractometer ( $\text{CuK}_\alpha$  radiation). The X-ray diffraction patterns were processed using the DRON-3 and ORIGIN-4 software programs.

The microstructure and morphological features of the quasicrystalline powders and coatings were examined on an MBI-15 optical microscope and a JEM-100C transmission electron microscope equipped with an EM-ASID-4 scanning adapter and an image processing system with the IMAGE-C software package.

The microhardness of the deposited quasicrystalline coatings was determined on a PMT-3 microhardness tester using the method of recovered indentation of a four-sided diamond pyramid.

The tribological tests were carried out on the upgraded SMT-1 friction machine according to the finger-disk scheme under conditions of dry friction.

The X-ray structural investigations of the initial powder and deposited coatings revealed that the coatings have a heterophase structure ( $\psi$ ,  $\beta$ ,  $\lambda$ ,  $\theta$  phases) with the competitive formation of the main phases, namely, the icosahedral  $\psi$  phase and the cubic  $\beta$  phase.

Figure 1 shows the X-ray diffraction patterns (filtered  $\text{CuK}_\alpha$  radiation) of the quasicrystalline coatings deposited at different temperatures of the substrate. It can be seen from this figure that intense diffraction peaks lie in the range of angles  $2\theta = 42^\circ\text{-}46^\circ$  and that the structure of the coatings is heterogeneous and consists of a mixture of two main phases: the icosahedral  $\psi$  phase and the cubic  $\beta$  phase. The influence of the substrate temperature  $T_k$  on the phase formation and structure of the deposited quasicrystalline coatings manifests itself as a change in the intensity ratio of the diffraction peaks corresponding to the  $\psi$  and  $\beta$  phases, for example, (422222), (110), and (420024).

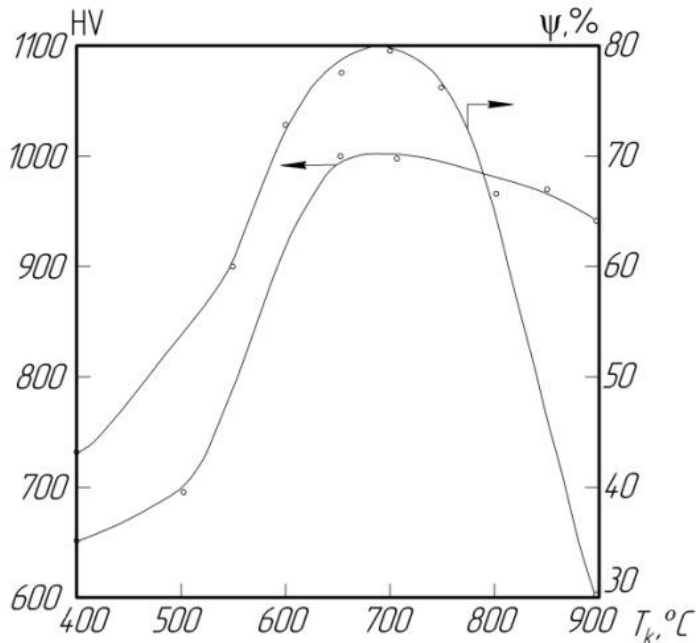


Fig. 2. Dependences of the microhardness HV and the weight content of the icosahedral  $\psi$  phase in the coatings on the substrate temperature  $T_k$  during the plasma spraying.

The weight content of the icosahedral phase in the deposited coatings was determined from the X-ray powder diffraction analysis data and the results obtained in [10, 22]. The calculated dependence of the weight content of the icosahedral phase in the coatings on the deposition conditions is shown in Fig. 2. It can be seen that, with an increase in the substrate temperature, beginning from  $T_k \sim 400$  °C, the fraction of the icosahedral phase increases, reaches a maximum near  $T_k \sim 700$  °C, and then decreases to 33% at  $T_k \sim 880$  °C.

Thus, the highest content of the icosahedral phase in the coatings (80%) is achieved upon their deposition on the substrates at a temperature of 600-750 °C.

The temperature conditions of the formation of quasicrystalline coatings are primarily responsible for their morphology. Figure 3 shows the cross sections of the coatings produced from the  $\text{Al}_{65}\text{Cu}_{23}\text{Fe}_{12}$  alloy at different substrate temperatures  $T_k = 500, 650,$  and  $850$  °C. It can be seen from this figure that the morphological pattern (microcracks and pores, their concentration, size, and distribution) depends substantially on the conditions of the formation of the coatings. In particular, at the substrate temperature  $T_k = 500$  °C (Fig. 3a), the coating is characterized by a large number of microcracks and cracks starting predominantly from the outer surface and, in some cases, extending through the entire thickness of the deposited layer. The pore formation nonuniformly occurs throughout the thickness of the coating, and the porosity reaches 20% near the substrate bottom and 10% on the free surface. In this case, an increase in the thickness of the coating leads to a decrease in the average pore size. In general, the pores have a rounded shape; however, near the inner surface of the deposited coating, there are pores that have an irregular shape and coalesce into microcracks [9, 11].

As the substrate temperature increases to  $T_k = 650$  °C, the morphological pattern of the cross section changes (Fig. 3b). The pores acquire a spherical shape, the average pore size decreases, and the pore volume distribution becomes more uniform. Moreover, as in the case of the substrate temperature  $T_k = 500$  °C, the coating also contains microcracks, even though to a lesser extent. Apparently, this is associated both with the specific features of the plasma spray technology and with the mechanical properties of the quasicrystalline alloy under investigation. Since the initial alloy has a high brittleness [4, 5], large internal stresses that are

characteristic of rapid quenching lead not to plastic deformation but to the appearance of microcracks and to brittle fracture of deposited particles, which is clearly seen in Fig. 3 at the substrate temperatures  $T_k = 500$  and  $650$  °C. The mechanism of the formation of long cracks arising on the side of the free surface of the deposited alloy coating is associated with the large shrinkage stresses generated during the rapid quenching under specified deposition conditions.

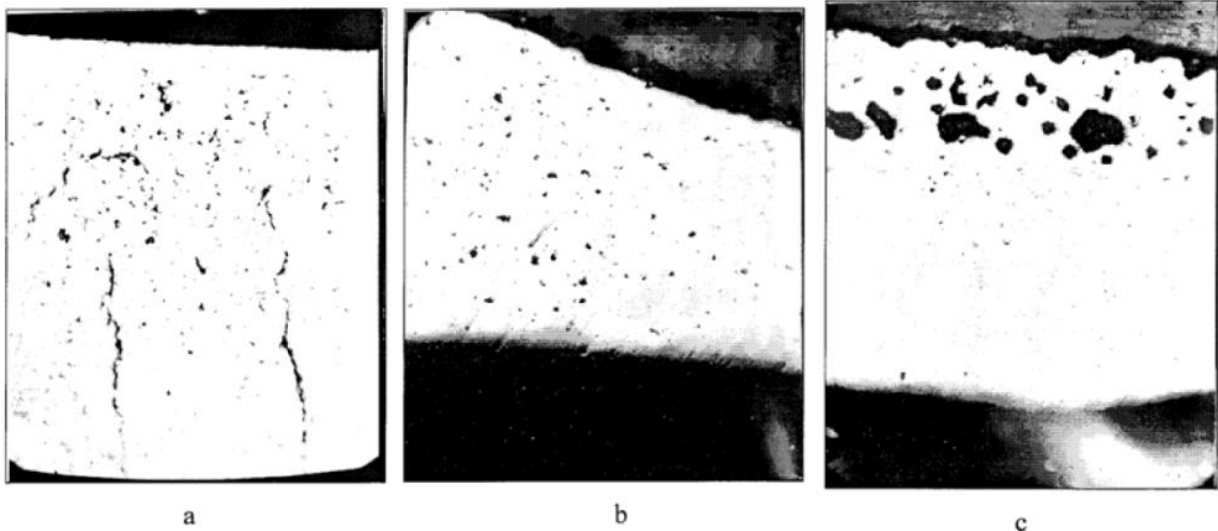


Fig. 3. Morphology of the cross section of the coatings (magnification,  $\times 90$ ) deposited at different substrate temperatures  $T_k = (a) 500$ ,  $(b) 650$ , and  $(c) 850$ °C.

At the substrate temperature  $T_k = 850$  °C, the surface of the coating undergoes melting. This process leads to the fact that, in the bulk of the deposited coating, typical pores either are absent at all or have very small sizes, less than  $1 \mu\text{m}$ . However, as can be seen from Fig. 3c, the alloy region near the free surface contains large pores of the bubble type with a size of  $80 \mu\text{m}$ . The appearance of this layer can be associated with the intensive process of gas release through the molten region of the coating.

In order to better reveal the microstructure of the coating, these samples were subjected to selective etching. The cross sections of the samples of the  $\text{Al}_{65}\text{Cu}_{23}\text{Fe}_{12}$  alloy coatings are shown in Fig. 4. It can be seen that the structure of these coatings is anisotropic and consists of uniform corrugated layers without foreign inclusions formed from molten particles, which is characteristic of the plasma spraying technology. The majority of the molten particles have a disk-like shape and are formed upon the deformation and solidification of the initial powder particles on the substrate, which were completely melted in the plasma. In addition, the coatings contain large particles, which were exposed to a high-temperature plasma jet but solidified before the collision with the substrate. The appearance of rounded small particles in the coating is caused by the spraying of larger droplets of the melt on the substrate. Furthermore, the deposited coatings contain particles of the mixed type, which combine features of several types of particles.

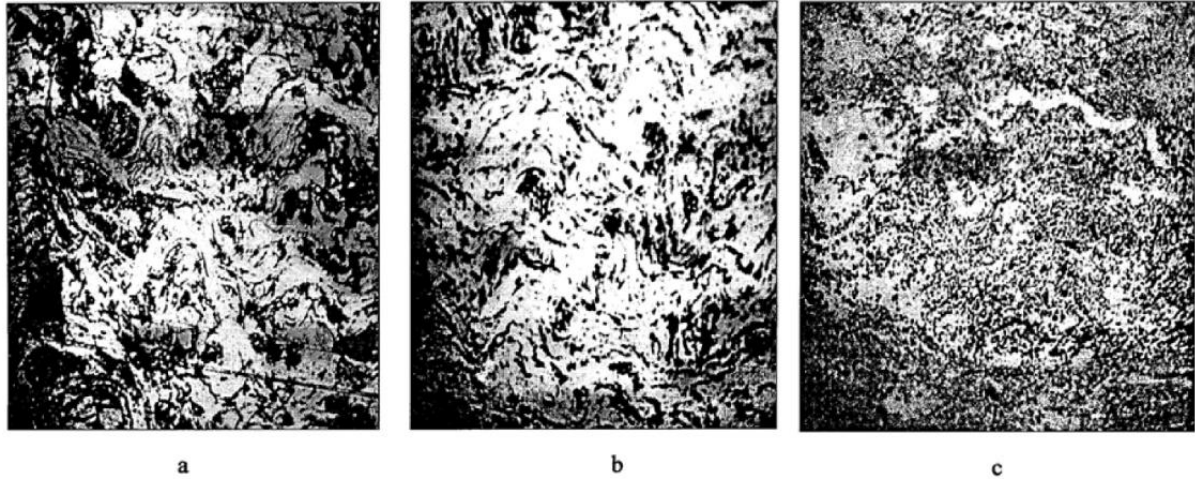


Fig. 4. Microstructure of the  $\text{Al}_{65}\text{Cu}_{23}\text{Fe}_{12}$  alloy coatings (magnification,  $\times 630$ ) deposited at different substrate temperatures  $T_k = (a)$  500,  $(b)$  650, and  $(c)$  850°C.

The interparticle layers formed during the deposition contain pores with the percentage of 6-10% depending on the conditions used for the preparation of the coatings. In particular, the coatings deposited at the substrate temperature  $T_k = 500$  °C are characterized by the lowest density. As the substrate temperature increases from  $T_k = 500$  °C (Fig. 4a) to  $T_k = 850$  °C (Fig. 4c), the corrugated structure of the coatings becomes denser, and the content of pores in the bulk of the material significantly decreases.

The microdiffraction pattern of the fracture surface of the deposited quasicrystalline coating consists of bright flat stepped regions. This pattern is characteristic of brittle fracture of the material. The cracking and fracture of the coating, as a rule, occur at the grain boundaries. A more detailed examination of the fracture surface revealed precipitates of individual powder particles and conglomerates forming the coating.

A comparative analysis of the microhardness was performed both on the initial quasicrystalline particles and on the deposited coatings based on them. The microhardness was determined on the polished surfaces of the samples with a roughness  $Ra = 0.34$  by the diamond pyramid with an indentation load of 50 g for individual particles and an indentation load of 100 g for the deposited coating. According to the results of the measurements, the initial quasicrystalline particles have a microhardness of the order of 850-900 HV. Such high values of the microhardness are determined by the non-porous monolithic structure and the sufficiently high content of the icosahedral phase ( $\sim 68\%$ ) in the bulk of the initial powders.



Fig. 5. Measurements of the microhardness on the cross section of the coating deposited at the substrate temperature  $T_k = 650$ °C (magnification,  $\times 630$ ).

The microhardness of the coatings was examined on the samples prepared under different deposition conditions and with different contents of the icosahedral phase. Figure 2 shows the combined dependences of the microhardness and the content of the icosahedral phase in the coatings on the temperature conditions of their deposition. It can be seen that the microhardness of the material increases both with an increase in the substrate temperature and with an increase in the weight content of the icosahedral phase. In particular, the microhardness of the coatings with a 80-percent content of the icosahedral phase reaches values of the order of 1000 HV. With a further increase in the substrate temperature  $T_k > 700$  °C, although the content of the icosahedral phase in the coatings decreases, their microhardness remains rather high. Apparently, this is associated with the formation of the molten layer and with the decrease in the porosity of the coatings.

Noteworthy is a significant increase in the brittleness of the Al-Cu-Fe alloy, which is evidenced by the tests on determination of the microhardness. After the indentation of a Vickers pyramid into the coating, radially directed cracks arise around the expression, which propagate mainly from the corners of the quadrangle.

The homogeneity of the properties of the deposited coatings was determined by analyzing the microhardness distribution in the cross sections of the samples. These measurements were performed on polished cross sections of the coatings with a step of 0.2 mm, beginning from the inner surface. The results of these investigations are presented in Fig. 5.

It can be seen that the structure of the indentations is identical almost over the entire thickness of the coating, which indicates a high uniformity of the deposited layers. The observed individual local overshoots of the values, most likely, can be explained by the fact that, during the measurements, the indenter falls into the interparticle space or into the region of pores of the deposited coating. The calculated values of the microhardness according to these indentations are presented in Fig. 6.

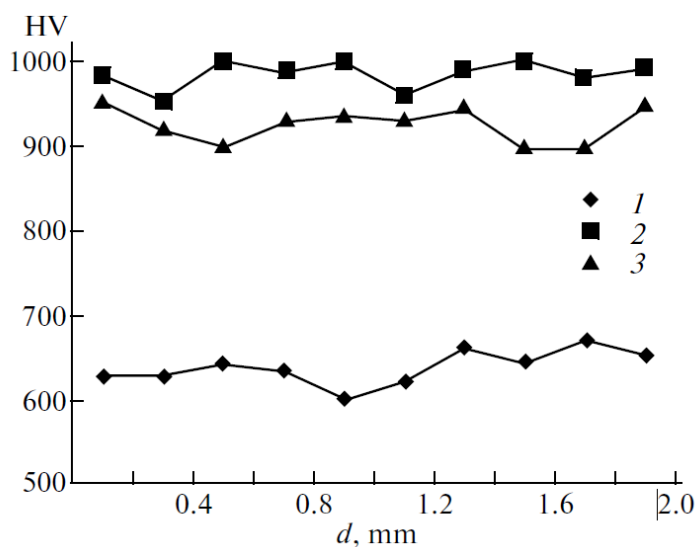


Fig. 6. Change of the microhardness HV in the cross section of the sample, beginning from the inner surface of the coatings deposited at different substrate temperatures  $T_k = (1)$  500,  $(2)$  650, and  $(3)$  850 °C.

The tribological (friction and wear) tests were carried out on the quasicrystalline coatings with the best combination of physical and mechanical properties, such as the content of the icosahedral phase, hardness, porosity, adhesion, etc.

The friction coefficient was determined using profilography with a Vickers pyramid

under a load of 30 N for the Al-Cu-Fe alloy coatings deposited at different substrate temperatures  $T_k$ . The performed investigations demonstrated that the friction coefficients of the deposited coatings differ only slightly from each other and their values lie in the range  $\mu = 0.15-0.20$  (Table 1).

Table 1. Friction coefficients of the quasicrystalline coatings prepared under different technological conditions of deposition

$T_k, ^\circ\text{C}$	400	500	650	750	850
Friction coefficient $\mu$	0,17-0,20	0,18-0,20	0,15-0,17	0,15-0,18	0,16-0,19

The somewhat larger friction coefficients, which are characteristic of quasicrystalline coatings deposited at  $T_k = 400-500^\circ\text{C}$ , can be explained by their higher porosity, lower content of the icosahedral phase, and microhardness.

The tests for wear resistance of the deposited coatings were carried out under dry friction conditions at different loads, wear rates, and wear times. The hardened steel ShKh15 was used as a counterbody.

It was found that the studied coatings possess a high wear resistance: the weight loss of the alloy was small and changed only slightly depending on the applied load, wear rate, and testing time (Fig. 7).

The morphological pattern of the coating surfaces after abrasion was smooth and did not exhibit grooves, adhesive wear traces, microcracks, and noticeable plastic deformation at the edges of the abrasion zone.

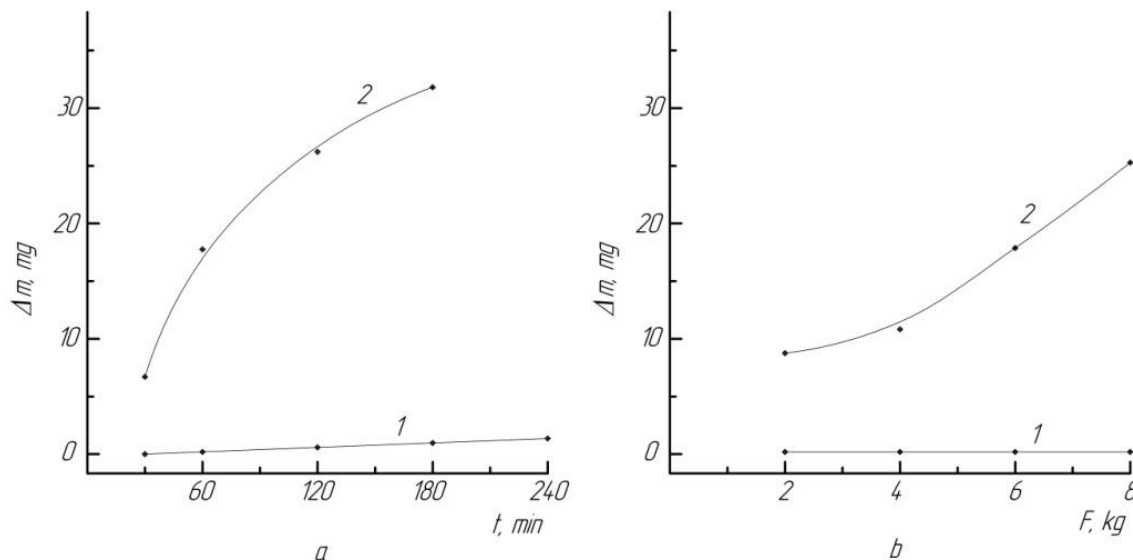


Fig. 7. Dependences of the weight loss of (1) the  $\text{Al}_{65}\text{Cu}_{23}\text{Fe}_{12}$  coating and (2) the titanium alloy VT 1-0 on the test time and (b) the applied load.

This behavior of the quasicrystalline coatings in testing for friction and wear differs significantly from the wear picture of the reference alloy VT 1-0 (Fig. 7, curve 2). The results of the tests performed for the VT 1-0 alloy under conditions similar to those used in the experiments with the Al-Cu-Fe coatings have demonstrated that, even in the early stages, an increase in the specific pressure leads to a sharp increase in the wear rate. The morphology of the worn surface of the titanium alloy is typical of severe plastic deformation with scratches, deep grooves, and traces of gripping and metal transfer. This eventually determined the low wear resistance of the titanium alloy VT 1-0 as compared to the quasicrystalline coatings.

The observed high level of wear resistance of the quasicrystalline coatings under dry friction conditions is associated with both the low value of the friction coefficient and the high hardness of the deposited alloy coating. Since the friction coefficients of the studied samples differ only slightly, the dominant role in the formation of high wear resistance, apparently, should belong to their high hardness.

Thus, from the practical point of view, the quasicrystalline coatings based on the Al-Cu-Fe alloy have important tribological characteristics under dry friction conditions. The technological principles underlying the preparation of such coatings are based on the justified choice of the chemical composition of the initial powders and the conditions of their deposition taking into account the regularities of the processes occurring in quasicrystalline alloys.

The morphological pattern of quasicrystalline coatings has a typical layered microstructure with a characteristic volume distribution of the pores and microcracks, which depends on the deposition conditions, in particular, on the substrate temperature  $T_k$ . The melting of the surface layer ( $T_k = 850^\circ\text{C}$ ) leads to a decrease in the porosity in the bulk of the coating and to an increase in the gas release through the molten layer.

The formation of the quasicrystalline coating is accompanied by the competitive interaction of two main phases, namely, the icosahedral  $\psi$  phase and the cubic  $\beta$  phase. As the temperature of the substrate increases, the fraction of the icosahedral phase first increases, reaches 80% at  $T_k = 700^\circ\text{C}$ , and then decreases to 33% at  $T_k = 880^\circ\text{C}$ .

It has been found that there is a correlation between the microhardness and the content of the icosahedral phase in the coating. The microhardness of the coatings increases with an increase in the content of the  $\psi$  phase and reaches  $\text{HV} = 900\text{--}1000$  when the content of the  $\psi$  phase is 80% ( $T_k = 700^\circ\text{C}$ ).

**Acknowledgments.** The work was performed with a support of the State R&D Task of the Ministry of Education and Science of the Russian Federation (Task No. 11.370.2014/K).

## References

- [1] Sordelet D, Rozhkova E, Besser M, and Kramer M 2002 *Intermetallics* **10**, 1233.
- [2] Sordelet D, Rozhkova E, Besser M, and Kramer M 2002 *Appl. Phys. Lett.* **80** 4735.
- [3] Yang X, Kramer M, Rozhkova E, and Sordelet D 2003 *Scr. Mater.* **49** 885.
- [4] Koster U, Liu W, Leibertz H, and Michel M 1993 *J. Non-Cryst. Solids* **153-154** 446.
- [5] Noskova N and Ponomareva E 1994 *Fiz. Met. Metalloved.* **78** 34.
- [6] Kronmuller H and Moser N 1988 *Z. Phys. Chem.* **157** 837.
- [7] Bratkovskii A, Danilov Y and Kuznetsov G 1989 *Fiz. Met. Metalloved.* **68** 1045.
- [8] Sordelet D, Kramer M. and Unal O 1995 *J. Therm. Spray Technol.* **4** 235.
- [9] Lepeshev A, Sordelet D, Rozhkova E and Ushakov A 2011 *J. of Cluster Sci.* **22** 289. doi: 10.1007/s10876-011-0378-2.
- [10] Karpov I, Ushakov A, Fedorov L and Lepeshev A 2014 *Technical Phys.* **84** 559. doi: 10.1134/S1063784214040148.
- [11] Ushakov A, Karpov I, Lepeshev A, Petrov M and Fedorov L 2014 *JETP Letters* **99** 99. doi: 10.1134/S002136401402009X.
- [12] Ushakov A, Karpov I, Lepeshev A and Petrov M 2015 *J. Appl. Phys.* **118** 023907. <http://dx.doi.org/10.1063/1.4926549>.
- [13] Lepeshev A, Karpov I, Ushakov A, Fedorov L and Shaikhadinov A 2016 *Intern. J. of Nanoscience* **15** 1550027.
- [14] Karpov I, Ushakov A, Lepeshev A and Zharkov S 2016 *Vacuum* **128** 123. doi: 10.1016/j.vacuum.2016.03.025.
- [15] Lepeshev A, Bayukov O, Rozhkova E, Karpov I, Ushakov A and Fedorov L 2015 *Phys.*



- of the Solid State* **57** 255. doi: 10.1134/S1063783415020249.
- [16] Ushakov A, Karpov I, Lipeshev A, Petrov M and Fedorov L 2015 *Phys. of the Solid State* **57** 919. doi: 10.1134/S1063783415050303.
- [17] Ushakov A, Karpov I and Lipeshev A 2015 *Phys. of the Solid State* **57** 2320. doi: 10.1134/S1063783415110359.
- [18] Fedorov L, Karpov I, Ushakov A and Lipeshev A 2015 *Inorg. Mater.* **51** 25. doi: 10.1134/S0020168515010057.
- [19] Lipeshev A, Karpov I, Ushakov A and Nagibin G 2016 *J. of Alloys and Compounds* **663** 631. doi:10.1016/j.jallcom.2015.12.168.
- [20] Rudenko K, Miakonkih A, Rogojin A, Bogdanov S, Sidorov V and Zelenkov P 2016 *IOP Conf. Ser.: Mater. Sci. and Engineering* **122** 012029. doi: 10.1088/1757-899X/122/1/012029.
- [21] Telegin S and Draganyuk O 2016 *IOP Conf. Ser.: Mater. Sci. and Engineering* **122** 012033. doi: 10.1088/1757-899X/122/1/012033.
- [22] Ebalard S and Spaepen F 1989 *J. Mater. Res.* **4**, 39.